AIMS Energy, 4(1): 173-189.
DOI: 10.3934/energy.2016.1.173
Received: 17 November 2015
Accepted: 28 January 2016
Published: 02 February 2016
Corrected: 19 March 2018

http://www.aimspress.com/journal/energy

Research article

Hydrothermal carbonization of glucose in saline solution: sequestration of nutrients on carbonaceous materials

M Toufiq Reza [1,2,3,*], Jessica Nover [4,5], Benjamin Wirth [3] and Charles J Coronella [2]

[1] Department of Mechanical Engineering, Ohio University, Ohio University, Athens, OH 45701, USA
[2] Department of Chemical and Materials Engineering, University of Nevada, Reno, 1664 N. Virginia Street, Reno, NV 89557, USA
[3] APECS Group, Leibniz Institute for Agricultural Engineering (ATB), Max-Eyth-Allee 100, Potsdam 14469, Germany
[4] Energy Process Engineering and Conversion Technologies for Renewable Energies (EVUR), Technische Universität Berlin, Fasanenstraße 89, 10623 Berlin, Germany
[5] Institute for Photovoltaics (ipv), University of Stuttgart, Pfaffenwaldring 4770569 Stuttgart, Germany

*** Correspondence:** Email: mreza@unr.edu; Tel: +1-775-784-4680; Fax: +1-775-327-5059.

Abstract: In this study, feasibility of selected nutrient sequestration during hydrothermal carbonization (HTC) was tested for three different HTC temperatures (180, 230, and 300 °C). To study the nutrient sequestration in solid from liquid solution, sugar and salt solutions were chosen as HTC feedstock. Glucose was used as carbohydrate source and various salts e.g., ammonium hydrophosphate, potassium chloride, potassium sulfate, and anhydrous ferric chloride were used as source of nitrogen and phosphorus, potassium, and iron, respectively. Solid hydrochar was extensively characterized by means of elemental, ICP-OES, SEM-EDX, surface area, pore volume and size, and ATR-FTIR to determine nutrients' sequestration as well as hydrochar quality variation with HTC temperatures. The spherical mesoporous hydrochars produced during HTC have low surface area in the range of 1.0–3.5 $m^2 g^{-1}$. Hydrochar yield was increased about 10% with the increase of temperature from 180 °C to 300 °C. Nutrient sequestration was also increased with HTC temperature. In fact, around 71, 31, and 23 wt% nitrogen, iron, and phosphorus were sequestered at 300 °C, respectively. Potassium sequestration was very low throughout the HTC and maximum 5.2% was observed in solid during HTC.

Keywords: Hydrothermal carbonization; glucose; hydrochar; nutrient sequestration; surface study; porosity

1. Introduction

Hydrothermal carbonization (HTC) has gained attentions from various scientific fields from solid fuel to carbon based catalyst and from waste treatment to low cost adsorbents over the last several years [1-9]. Because of its very high ionic product [10], when biomass is treated with subcritical water (200–280 °C), organic components of the biomass degrade and re-polymerize into solid hydrochar. Hydrochar is hydrophobic, energy dense, carbon-rich amorphous solid, although the quality depends on HTC reaction parameters as well as raw feedstock [11-13]. In addition to fuel application, hydrochar's potential for soil amendment, slow release fertilizer, and carbon sink have been evaluated by several research groups around the world [8,14].

Several publications have already reported the fate of elemental nitrogen, phosphorus, and potassium during HTC from various feedstocks including lignocellulosic or waste biomass [2,15,16]. In fact, a recent article discussed about the fate of plant available nutrients in the form of NH_4^+ and PO_4^{3-} during HTC of digestate [14]. During HTC, nitrogen could be recovered either as HTC process liquor or distributed evenly in hydrochar and liquid phase [16,17]. The difference in feedstock as well as the different reaction condition makes the comparison unrealistic. Phosphorus has been recovered primarily in hydrochar, although there are several cases, where majority of the phosphorus was found in liquid phase [2,15]. In contrary, most literatures agree with the fate of potassium in the process liquid [2,14,16]. It is impossible to discuss the opposing reports because different feedstocks, experimental setups, and reaction conditions have been applied. However, all of these literatures failed to explain the nutrient recovery phenomena.

The HTC reaction chemistry has been evaluated very extensively studying both model compounds and various biomass feedstocks [12,18-20]. There are evidences of chemisorption sites on the hydrochar [21], which makes hydrochar effective for chemisorption of selective substances like U(VI), Cu, Cd, triclosan etc. [22-25]. However, the sorption phenomena for plant available nutrients (N, P, K) need further investigation. It is still unknown whether the nutrients in the solid hydrochar are resulted from nutrient adsorption or nutrient remaining due to the incomplete degradation of fiber components.

The main goal of this study was to find out whether nutrients are sequestered during HTC. The term sequestration can be defined for this study as the nutrients uptake on the hydrochar during HTC. To eliminate nutrients sorption from the feedstock nutrients, glucose solution has been used as feedstock. Various salts containing targeted nutrients (NPK) are used as nutrient sources. Investigations of specific nutrient contents as well as their positions on hydrochar are explained here. Moreover, a simple reaction mechanism is proposed and discussed in this article.

2. Materials and Methods

2.1. Materials

All the salts (potassium chloride, ammonium hydrophosphate, potassium sulfate, and anhydrous ferric chloride) and sugar (glucose) were purchased from VWR, Germany. The salts and sugar were more than 98% pure. Rest 2% of the salts is impurity including copper, chromium, calcium, aluminum, and cobalt. Individual 1 M solutions of all sugar and salts are produced using de-ionized water and are stored in a sealed glass bottle until HTC.

2.2. Hydrothermal carbonization

In a HTC experiment, 60 mL of 1M glucose solution, 10 mL of 1M KCl, 10 mL of 1M $NH_4H_2PO_4$, 10 mL of 1M K_2SO_4, and 10 mL of 1M $FeCl_3.6H_2O$ were poured in a 200 mL Parr pressure bomb (Parr model 4570, Moline, IL). The experimental condition was set to 180, 230 or 300 °C for holding time 16 h with 3 K min^{-1} heating rate. According to the previous studies, HTC reactions, especially in the liquid state, requires several hours to complete depending on the reaction parameters [8,19,31]. To ensure the completion of the HTC reaction, a very long reaction time (16 h) was chosen for this study. After the end of reaction period, the heater was turned off and let the reactor cooled down naturally. It took 3–4 h to cool down from 300 °C to 25 °C (about 30–45 min from 300 °C to 180 °C). The gaseous product was purged in the fume hood; hydrochar was filtered using a folded filter paper (ROTH Type 113 P filter) for 20 min and washed with excess de-ionized water for another 10 min to remove physically adhered nutrients on the surface. Hydrochar was dried in a heating oven at 105 °C for overnight. Dried hydrochar was placed into a zip-lock bag and stored for further physico-chemical analyses. All the experiments were at least duplicated for this study. Hydrochars were named as HTC-T, where HTC stands for hydrothermally carbonized char and T is the HTC temperature, respectively.

2.3. Product characterization

Elemental carbon, hydrogen, nitrogen, and sulfur (CHNS) were measured using a Vario El elemental analyzer (Elementar Analysesysteme Hanau, Germany). Sulphonic acid was used in this elemental analysis as reference and two ovens were set at 1150 °C, and 850 °C, respectively. Each sample was analyzed three times, and average elemental compositions are reported.

A Nicolet iS5 ATR-FTIR (Thermo Scientific, Madison, WI, USA) with mid- and far-IR capabilities was used on the raw and hydrothermally treated biomass. IR spectra of all solid samples were recorded at 30 °C using ATR-FTIR. All samples were milled into fine powder for homogenize and dried in 105 °C for 24 h in an oven prior to FTIR. Only 5–10 mg of dry sample was placed in the FTIR for this analysis and pressed against the instrument's diamond surface with its metal rod. All spectra were obtained using 64 scans for the background (air) and 64 scans for the samples, which were scanned from 500–4000 cm^{-1}.

The morphology of samples HTC-180, HTC-230, and HTC-300 were analyzed using SEM-EDX and nitrogen adsorption. For SEM, hydrochar samples were dispersed on a conductive pad and introduced into the SEM equipment. The investigation was carried out using a Cambridge S200 scanning electron microscope (SEM) at an excitation voltage of 20 kV and a sample distance of 18 mm. The SEM samples were prepared by depositing about 50 mg of dry powdered hydrochar on an aluminum stud covered with carbon conduction tapes, and then coated with Pt for 1 min to prevent charging during observation.

The specific surface area was determined based on nitrogen adsorption at 77 K and the BET method according to ISO 9277. Barrett-Joyner-Halenda (BJH), Dubinin-Radushkevich (DR), Horvath-Kawazoe (HK), and Non-Local Density Functional Theory (NLDFT) methods were used to determine the volume of meso- and micropores according to DIN 66134 and DIN 66135, respectively. Hitachi scanning electron microscope (SEM) S-2700 was used to investigate the influence of the process setting on hydrochars' microscopic structure.

Targeted nutrients (potassium and phosphorus) and trace elements (aluminum, calcium, cobalt, chromium, copper, iron, magnesium, manganese, sodium, nickel, sulfur, and zinc) were determined by an induced coupled plasma optical emission spectrometry (ICP-OES). The hydrochar samples were digested by nitric acid (ACS grade, 65% pure) and hydrogen peroxide (10% pure) at 250 °C for 20 min in a MWS 640 microwave (MLS GmbH, Germany). For ICP-OES, an iCAP 6000 analyzer from Thermo Fisher Scientific, Inc. USA was used for inorganic determination.

3. Results and Discussion

3.1. Chemical analyses of hydrochars

A series of HTC experiments were conducted on glucose solution in presence of various salts and varying HTC temperature. The salt and sugar concentration in the feed was maintained similar to find out the HTC temperature effect on nutrient sequestration. As HTC of glucose as model compound was reported from 180–250 °C [24,26-29], two different HTC temperatures (180 and 230 °C) and one higher temperature (300 °C) were chosen for this study. The long reaction time (16 h) was chosen to ensure the completion of HTC reactions even at the lowest temperature (180 °C). It was previously reported that the presence of iron catalyze in favor of hydrochar during HTC process [21,30]. Moreover, iron itself is an essential micronutrient for plant growth. Hence, iron salt was added with others for nutrient sequestration in hydrochar. As nutrient sequestration is the main objective of this study, the process liquid and the gaseous product were not further studied. Solid production (weight of solid hydrochar product from 100 mL of feedstock), ultimate analysis (CHNS), and selective nutrient elements are reported in Table 1.

Nutrient sequestration on the hydrochar during HTC can be seen from Table 1. All the nutrients (N, K, and P) at different concentrations have been found in the hydrochar. As the starting HTC feedstock was liquid solution of sugar and salts, formation of hydrochar during HTC with nutrients proves that nutrients from the liquid streams can be sequestered in the solid hydrochar during HTC. It can also be found from Table 1 that solid recovery was increased with HTC temperature. According to the previous studies [26,28,31,32], HTC temperature above 180 °C has minimal effects on glucose-derived-hydrochar production for an extended HTC reaction time. In other words, carbon in hydrochar, once produced from glucose, is fairly stable under subcritical water. In fact, the elemental carbon content from Table 1 implies the consistent result in this study. Now, an increase of mass yield indicates either an increase of nutrients in hydrochar with the increase of HTC temperature, or the salts catalyze HTC reaction and catalytic activity increases with HTC temperature, or both.

If the mass yield is expressed as mass of hydrochar produced from mass of salt and sugar input, then the mass yield become 53.3, 55.6, and 64.5% in HTC-180, HTC-230, and HTC-300, respectively. Moreover, the carbon yield (ratio of carbon (g) in product and carbon (g) in feedstock) is very similar to the overall mass yield. In fact, it was reported earlier that only mass yield or solid production is around 50-53% of the overall mass when glucose was hydrothermally carbonized from 180–250 °C for 1–16 h [33,39]. Unlike the previous study, the mass yield increases with HTC temperature. The carbon concentration remains similar, which means that the overall mass of the carbon along with the nutrient concentrations increase in hydrochar with HTC temperature.

Unlike carbon, nitrogen concentration in the hydrochar was increasing with HTC temperature as well. In terms of mass recovery of nitrogen, around 61.5–71 wt% of nitrogen was sequestered on hydrochar and mass of nitrogen in the hydrochar increases with HTC temperature. Other nutrients e.g., iron, potassium, sulfur, and phosphorus show an increasing trend of their concentration on hydrochar with the increase of HTC temperature. Similar increase of nutrients can be observed from previous study [40]. The nutrients did not follow a linear relationship; however, overall they increase with the increase of HTC temperature from 180 °C to 230 °C. The increment of temperature above 230 °C further sequester several nutrients, while the others like potassium remains similar. Potassium may have reached the maximum sequestration at around 230 °C. Among these nutrients, iron and sulfur concentration increases about two times from HTC-180 to HTC-300. In terms of mass recovery, mass of iron sequestration increases from 8.6 wt% to 31.5 wt% in HTC-180 to HTC-300 hydrochar. Phosphorus concentration also increases about 87 % from HTC-180 to HTC-300. Phosphorus sequestration on hydrochar increases from 10.1 wt% to 23 wt% in HTC-180 to HTC-300. Unlike nitrogen, iron, and phosphorus, potassium sequestrations in hydrochar was very low. In fact, only 3.0–5.2 wt% of potassium was recovered in hydrochar and the highest recovery was observed in HTC-230. Potassium, available as potassium ion (monovalent cation) in liquid, has the highest dissociation constant among the other nutrients. As a result, potassium has the tendency to remain in the liquid even during HTC.

Table 1. Solid recovery, elemental CHNSO, and nutrients of hydrochar produced at different HTC temperatures.

Hydrochar	Solid production[1] (g per 100 mL)	Mass yield (g $g^{-1}_{\text{dry reactants}}$)	Elemental analysis[2]					ICP-OES[3]			
			Nitrogen (%)	Carbon (%)	Sulfur (%)	Hydrogen (%)	Oxygen (%)[4]	Iron (mg kg^{-1})	Potassium (mg kg^{-1})	Phosphorus (mg kg^{-1})	Sulfur (mg kg^{-1})
Dry reactants	NA	1.0	1.4	23.3	2.3	4.2	68.8	55,800	117,194	31,000	23,593
HTC-180	9.1 ± 0.5	0.53 ± 0.04	0.9	62.7	0.2	4.5	31.7	5271	3800	3424	533
HTC-230	9.5 ± 0.4	0.56 ± 0.04	1.0	64.0	0.2	4.5	30.3	8920	6389	5346	790
HTC-300	11.1 ± 0.5	0.65 ± 0.06	0.9	63.1	0.3	3.9	32.4	15,621	6309	6412	1579

[1] $Solid\ production = \frac{mass\ of\ hydrochar\ dry\ (g)}{Total\ volume\ of\ feed\ (ml)} \times 100$

[2] Precision of the elemental analysis is ±0.5 wt%

[3] Precision of the ICP-OES is 100 mg kg^{-1}

[4] % O = 100 – (%C + %H + %N + %S); NA: Not applicable

3.2. Porosity properties of hydrochars

N_2 adsorption-desorption isotherms for HTC-180, HTC-230, and HTC-300 are shown in Figure 1. The adsorption isotherms of the hydrochars, regardless of the activation conditions, showed type IV isotherms, indicating presence of large fractions of mesoropores [31]. HTC-180 and HTC-230 show more mesopores than HTC-300. The N_2 adsorption isotherms in Figure 1 showed that there is a significant downward shift in N_2 adsorption for all samples, due to the effect of heat shrinking and oxidation and decomposition of the products. The trend is similar as found in the desorption isotherms. The increase of nutrient concentration in the hydrochar may decrease the gas uptake even at higher pressure. The similar phenomenon was observed and reported in a previous study [29], where zinc chloride and lithium chloride eutectic salts are used during HTC of glucose at 180 °C.

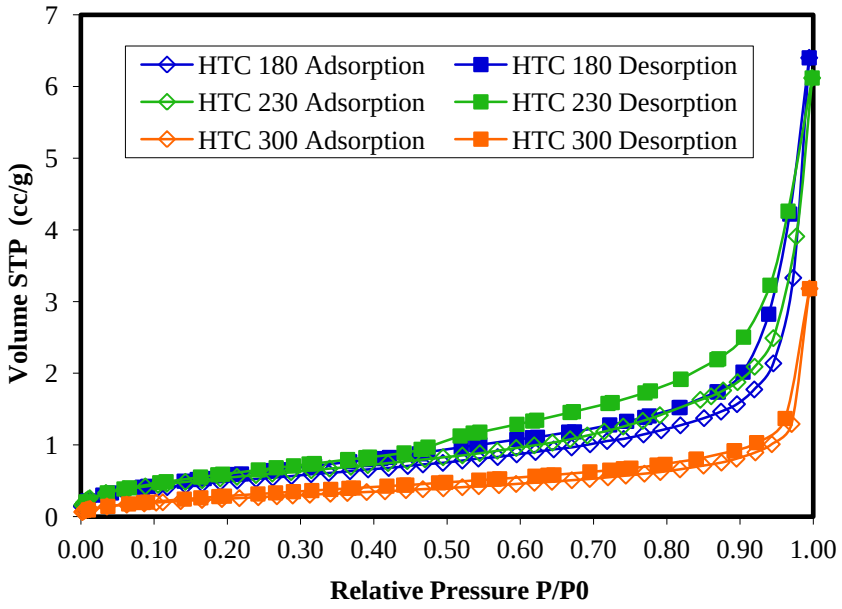

Figure 1. Nitrogen sorption isotherms of HTC-180, HTC-230, and HTC-300 hydrochars.

Lower gas uptake might also be caused by the smaller particle size, which might indicate that the average particle size reduces with HTC temperature. Surface area, pore size, and pore volume were calculated in various methods and the results are listed in Table 2. All the hydrochars have very similar multipoint BET surface area in the range of 1.0–3.5 $m^2 g^{-1}$. However, the BJH and DH surface areas are highest for HTC-180 (BJH and DH adsorption surface area 8.0 and 8.1 $m^2 g^{-1}$, respectively) and lowest for HTC-300 (BJH and DH adsorption surface area 3.8 and 3.9 $m^2 g^{-1}$, respectively). This might be the reason for less pronounced gas uptake by HTC-300 than HTC-180.

The pore volumes are presented in the Table 2 as well. With the lower BJH surface area, it is expected that the pore volume would be lower which is observed in Table 2. In fact, the BJH and DH pore volume of HTC-300 were around 50% lower than those of HTC-180. Average pore size was very similar for all the hydrochars. In fact, pore size of hydrochars determined by BJH, DH, HK, and SF were around 0.18–0.56 nm. HTC-300 was predominantly mesoporous, as can be found from the NLDFT pore size for HTC-180 and HTC-230 were both 20.09 nm.

From the porosity analysis, it can be concluded that all the hydrochars are mesoporous, which is different than pyrolysis biochar [34]. In biochar, physisorption is more dominant, as the large

microporous surface area. However, hydrochar seems to have very low BET surface area and it is mostly mesoporous. Therefore, in the case of nutrient sequestration, it should be chemisorbed with the chemically active sites on the hydrochar surface. To find out the chemisorption sites on the hydrochar surface and possible nutrient bonding with hydrochar carbon, FTIR was carried out for all the hydrochars and the results are discussed below.

Table 2. Surface area, pore volume, and pore size analysis of hydrochars using various methods.

Morphology	Method	HTC-180	HTC-240	H-300
Surface area ($m^2\ g^{-1}$)	Multi point BET	1.85	2.05	0.98
	BJH method cumulative adsorption surface area	7.96	8.26	3.80
	BJH method cumulative desorption surface area	5.47	6.44	2.96
	DH method cumulative adsorption surface area	8.08	8.40	3.87
	DH method cumulative desorption surface area	5.65	6.68	3.07
	t-method external surface area	1.85	2.05	0.98
	t-method micropore surface area	1.81	ND	ND
	NLDFT cumulative surface area	0.00	2.01	0.89
Pore volume ($mL\ g^{-1}$)	BJH method cumulative adsorption pore volume	1.10×10^{-2}	1.11×10^{-2}	5.70×10^{-3}
	BJH method cumulative desorption pore volume	1.11×10^{-2}	1.08×10^{-2}	5.54×10^{-3}
	DH method cumulative adsorption pore volume	1.06×10^{-2}	1.08×10^{-2}	5.52×10^{-3}
	DH method cumulative desorption pore volume	6.89×10^{-4}	1.05×10^{-2}	5.38×10^{-3}
	t-method micropore volume	ND	ND	ND
	HK method cumulative pore volume	6.89×10^{-4}	7.65×10^{-4}	3.47×10^{-4}
	SF method cumulative pore volume	7.11×10^{-4}	7.89×10^{-4}	3.60×10^{-4}
	NLDFT method cumulative pore volume	5.45×10^{-3}	5.73×10^{-3}	1.94×10^{-3}
Pore size (nm)	Average pore Radius	10.71	9.23	10.05
	BJH method adsorption pore Radius (Mode dV(r))	0.45	0.46	0.45
	BJH method desorption pore Radius (Mode dV(r))	0.55	0.55	0.56
	DH method adsorption pore Radius (Mode dV(r))	0.45	0.46	0.45
	DH method desorption pore Radius (Mode dV(r))	0.55	0.55	0.56
	HK method pore Radius (Mode)	0.34	0.18	0.18
	SF method pore Radius (Mode)	0.18	0.18	0.23
	NLDFT pore Radius (Mode)	20.09	20.09	0.75

ND: not determined

3.3. FTIR spectroscopy of hydrochars

FTIR spectroscopy has been extensively used in biomass research, as it shows the bond energies of characteristic groups in biomass, and can indicate changes in molecular formation resulting from various treatments [12]. The FTIR spectra of raw glucose, and different hydrochars were performed and the spectra are shown in Figure 2. Raw glucose shows strong bonds at 896, 1036, 1186, 1244, 1367, 1426, 1618, 2845, and 3300 cm^{-1} in the spectrum. These correspond to carbon hydrogen bond (C-H), alcohol group (C-OH), aryl-alkyl ether (C-O-C), organic acid (-COOH), carbon skeleton (C=C), carbon hydrogen bond (C-H), and hydroxyl bond (-OH), respectively [12, 32]. With HTC, oxygen containing bonds in hydrochars are deemed mainly because the volatile oxygen-rich components degrade into liquid and gaseous products [12].

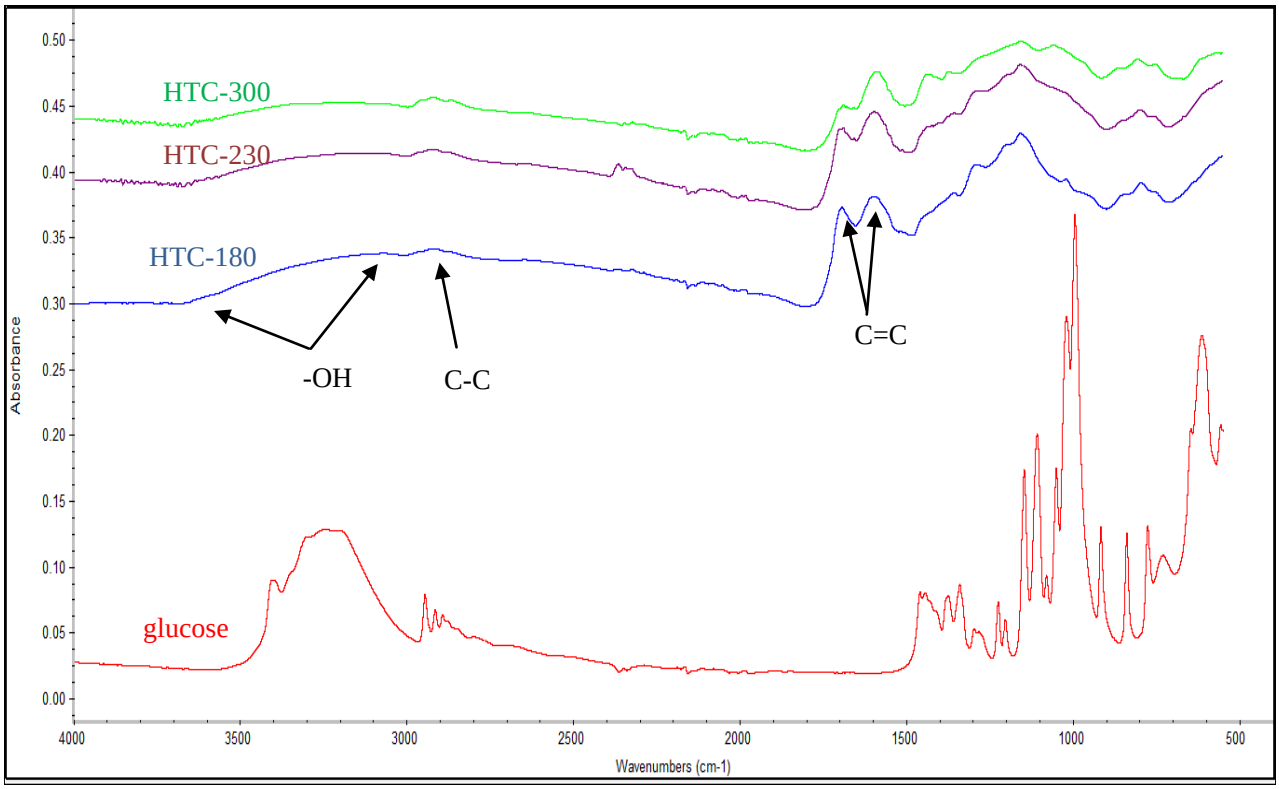

Figure 2. (from bottom to top) IR spectroscopy of raw glulose, HTC-180, HTC-230, and HTC-300 hydrochars. Note: y-axis has arbitrary units.

The elemental analysis, presented in Table 1, shows an increase of elemental carbon, also in complement with the FTIR spectra. Two new peaks at 1600 and 1700 cm^{-1} corresponding to C=C bonds are produced and sharpen for all hydrochar spectra. This might be another confirmation of carbonization during HTC as previously addressed by various researchers [12,35]. Besides C=C bonds, there is also evidence of organometallic bonds e.g. C-N or C-P bonds in 1030 cm^{-1}, C=S bond in 1170 cm^{-1}, $-NH_2$ or $-CH_2$ twist in 1350 cm^{-1} etc. In addition, two shifted peaks observed at 745 and 830 cm^{-1} further confirmed the formation of C-O-Fe bonds due to the interaction between iron and the carbon matrix. They were related to Fe-O stretching modes of the tetrahedral and octahedral sites in its spinel structure [36]. Supporting the ICP-OES results in Table 1, the iron and phosphorous bonds were sharpening with HTC temperature. Thus, combining the elemental analysis

and FTIR indicates the formation of nutrient containing carbon spheres during HTC of glucose with salt addition. SEM-EDX may reveal the sites and distribution of nutrients on the hydrochar surface.

3.4. SEM-EDX investigation of hydrochars

It is important to know whether the nutrients chemisorb on the hydrochar or they formed inorganic salts during the cooling phase. One can only speculate from porosity analysis that the nutrients are probably chemisorbed on the hydrochar as the physisorbed salts may have been washed away during washing after hydrochar production. However, to prove this as well as to find the effect of various nutrient concentrations in hydrochar formation, SEM-EDX was performed in all three hydrochars. SEM images are reported in Figure 3, whereas elemental scanning for HTC-180, HTC-230, and HTC 300 is presented in Figures 4, 5, and 6, respectively.

From Figure 3, carbon spheres formed during HTC can be observed. The starting feedstock was glucose dissolved in saline solution. The spheres were nucleated and developed during HTC. The similar carbon spheres produced during HTC of saccharides were previously reported [25-27,31]. It has also been reported that the size of carbon spheres are around 1 ± 0.8 μm, when glucose was hydrothermally carbonized from 170–240 °C for 1–15 h [31]. The carbon spheres produced in this study are clearly larger compared to that previous study. In fact, a higher degree of aromatization was reported earlier in the presence of eutectic salt solution during HTC of polysaccharides [29]. The presence of salts during HTC yield higher energy value, according to another study [37]. In fact, iron in the solution might catalyze the HTC and probably nucleate the formation of carbon spheres. As a result, the carbon spheres are larger and contain nutrients in their structure, which can be observed from the EDX.

Elemental scanning or EDX was performed to find out the nutrients distribution on the hydrochar's surfaces. Elements of interest for this study are carbon, oxygen, phosphorus, potassium, and iron along with other possible inorganics (due to their presence in the salts) distribution in HTC-180, HTC-230, and HTC-300 are presented in Figures 4, 5, and 6, respectively. As carbon tape was used to attach the hydrochar in the stud during SEM-EDX, carbon can be observed on the other sites besides the samples as well. From Figure 4–6, carbon and oxygen were dominating in the hydrochars, regardless of HTC temperature. Phosphorus and iron were very widely distributed in all of the hydrochars. As discussed earlier (section 3.1), potassium is unlikely to chemisorb in the solid hydrochar during HTC, there is no visible evidence of potassium in the EDX of hydrochars at any HTC temperature. Chromium, the impurity of iron salt was also visible in the EDX in all hydrochars as well. According to Table 1, sulfur concentration increases around three times in HTC-300 than HTC-180. As a result, there is some evidence of sulfur in the EDX of HTC-300 hydrochar.

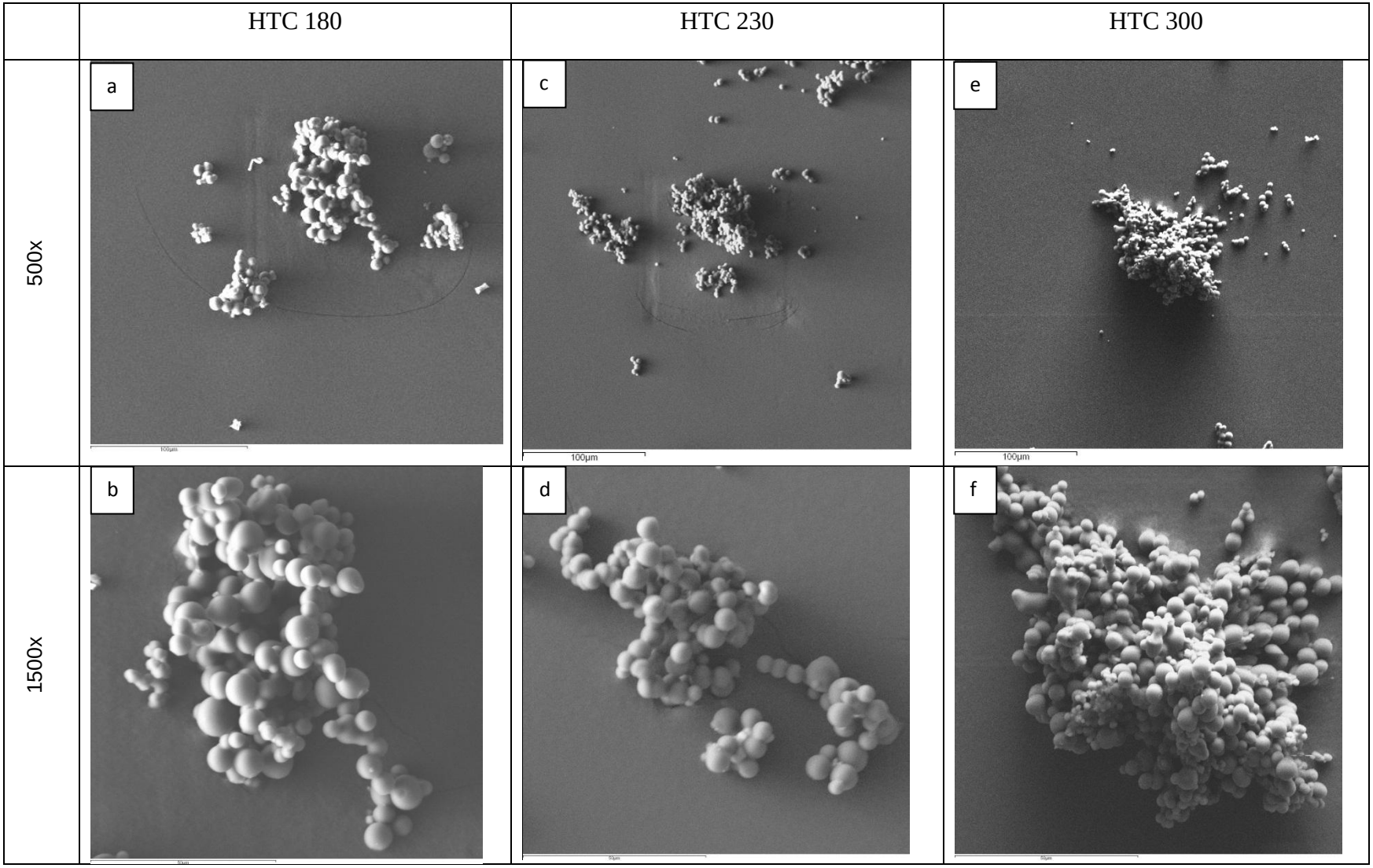

Figure 3. SEM images of HTC-180 (a,b), HTC-230 (c,d), and HTC-300 (e,f) hydrochars in lower (500x) and higher (1500x) magnification, respectively.

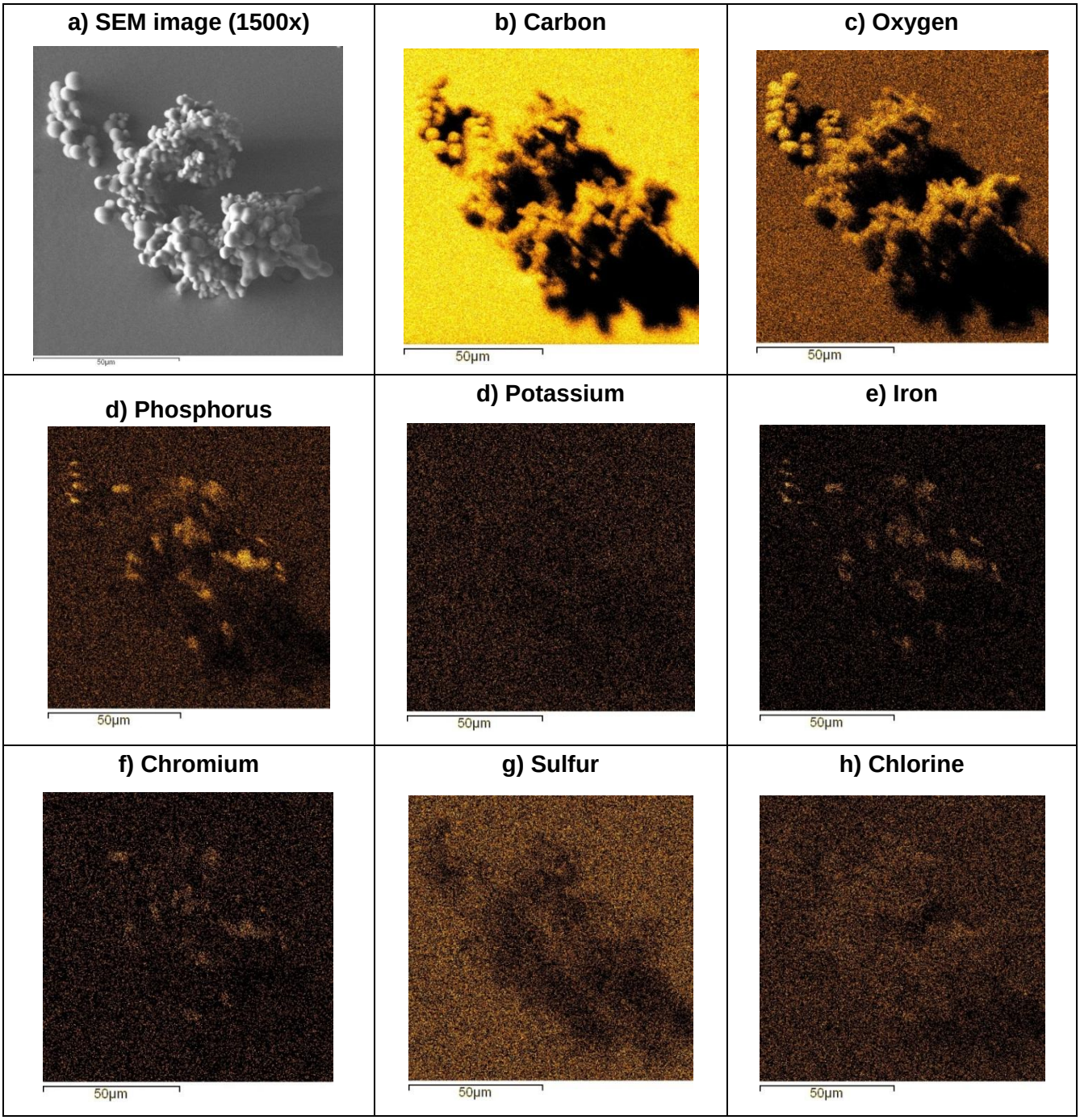

Figure 4. Elemental scanning of HTC-180 hydrochar.

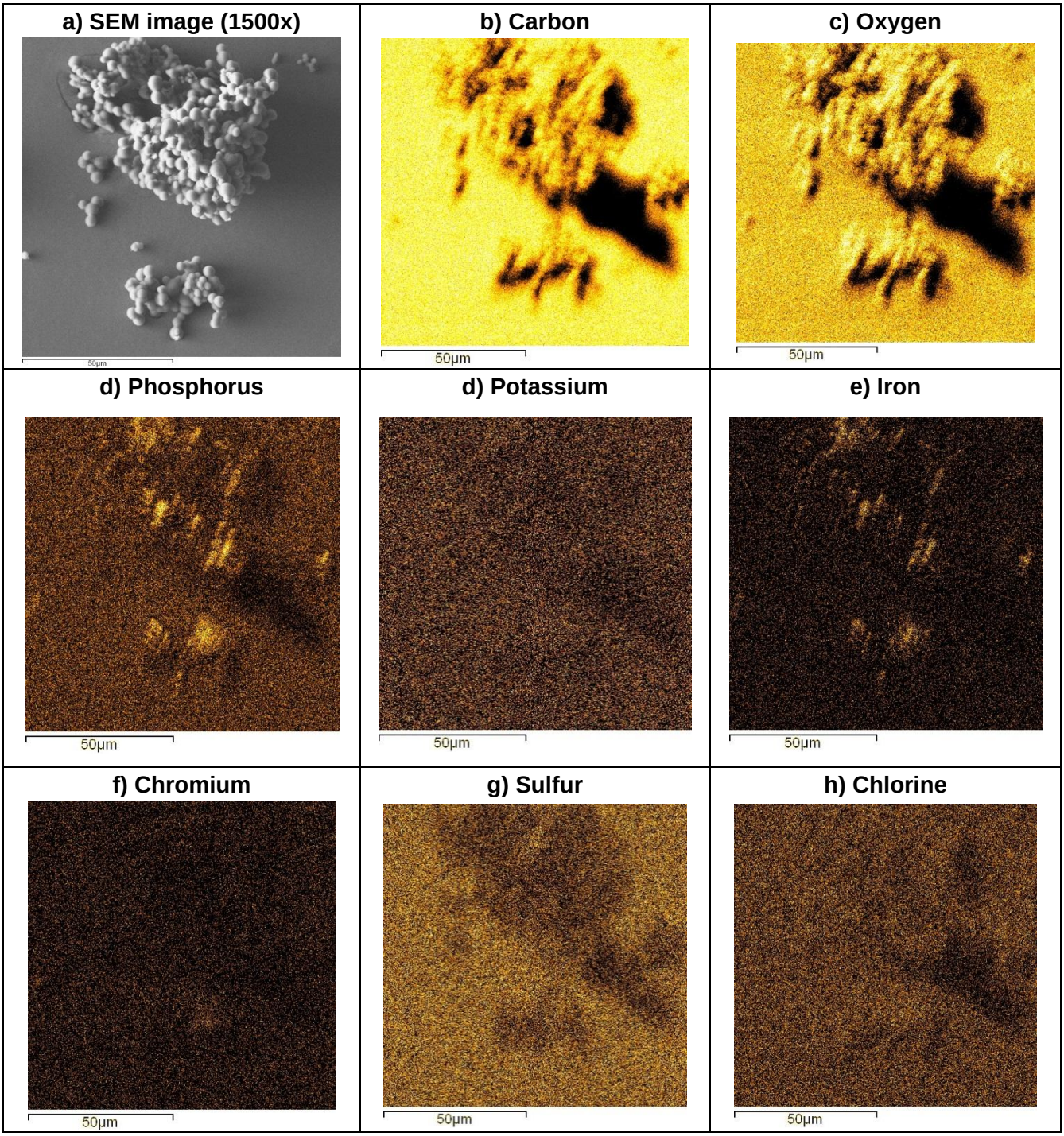

Figure 5. Elemental scanning of HTC-230 hydrochar.

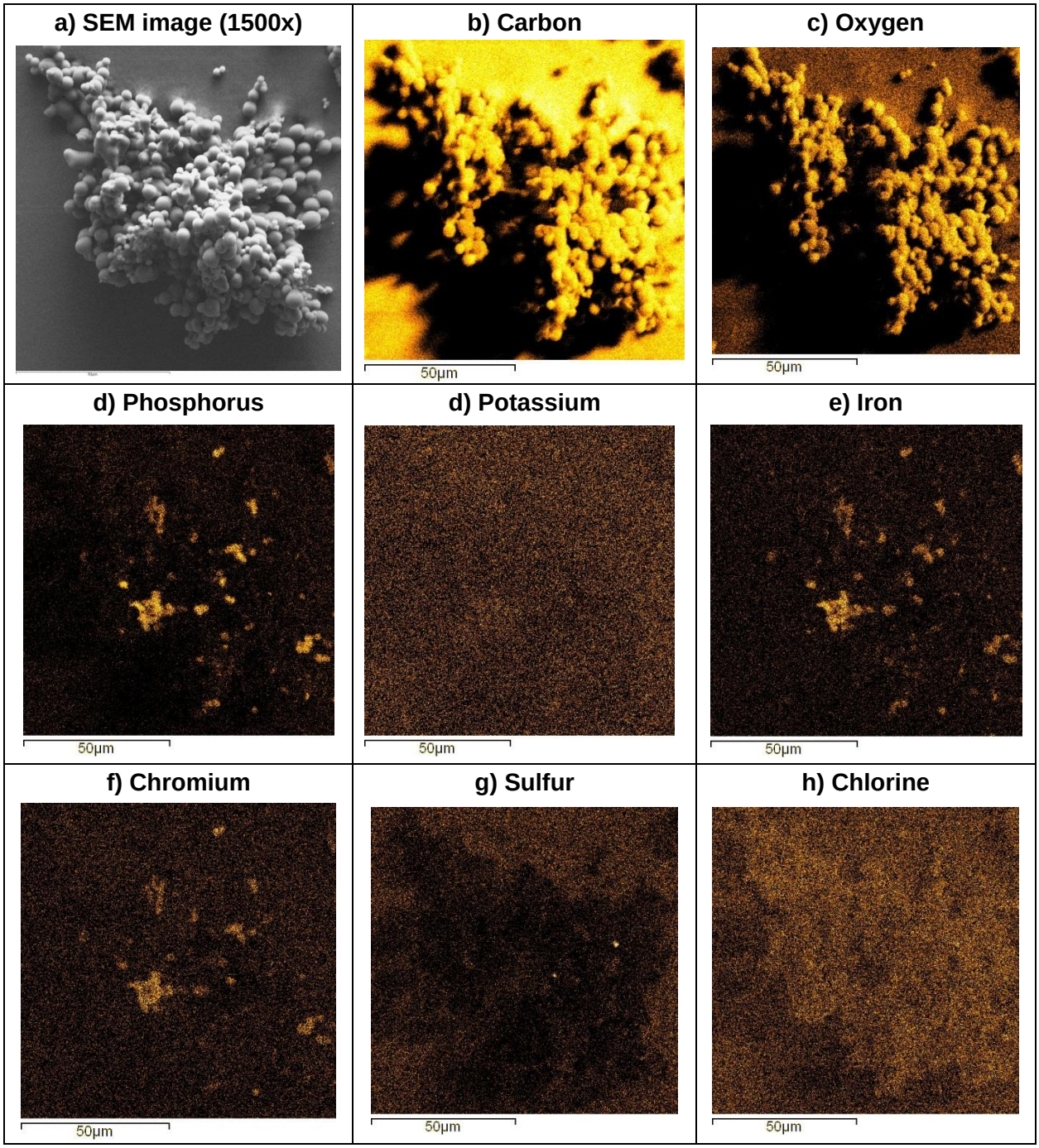

Figure 6. Elemental scanning of HTC-300 hydrochar.

3.5. Formation of nutrient sequestered carbon particles

A number of studies has been reported the HTC reaction pathways to produce hydrochar from model compounds (e.g., sugars, cellulose) to real biomass (e.g., wood) [18,20,31,38]. Regardless of the feedstock type, four major HTC reactions occur in this following sequence: (i) dehydration of sugars into furan compounds, (ii) polymerization or condensation of furan-derivatives, (iii) aromatization of polymerized products, and finally (iv) solidification of macromolecules into macromolecules [33,38]. Based on the FTIR results previously explained in Section 3.3, it is evident that similar reaction

mechanism takes place for sugar molecules with the presence of salinity as well. In addition, nutrient sequestration on the surface take place via chemisorption. The complete reaction mechanism is shown in Figure 7. Previously, it was reported that hydrochar spheres consist of a hydrophobic core and hydrophilic surface with various oxygen functional groups [18,31]. Due to their charge density, these functional groups (esters, acids, ketones etc.) are behaving as chemisorption sites (section 3.3) [22,23]. Charged nutrient molecules (NH_4^+, PO_4^{3-}) are attracted by the surface sites and adsorb as shown in Figure 7. These functional groups on the surface chemisorb nutrient ions, which are also found from FTIR spectra. The longer reaction temperature results more functional groups on the solid surface. Therefore, more nutrients are sequestered on the hydrochar surface.

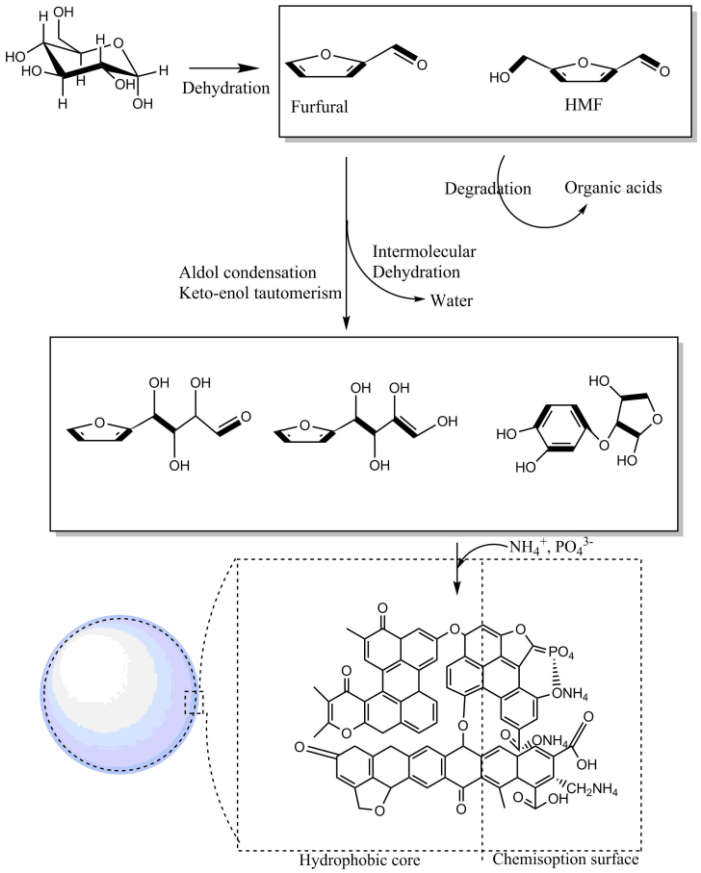

Figure 7. Mechanism of the formation of nutrient sequestered carbon particles from glucose in saline solution [33,38].

4. Conclusions

In presence of saline solution, hydrochar yield from glucose increases with HTC temperature, although carbon concentration in the hydrochar remains similar. Maximum 71, 31, and 23.1 wt% nitrogen, iron, and phosphorus respectively were recovered in solid hydrochar at highest HTC temperature (300 °C). Potassium was unlikely to be recovered in solid during HTC in the temperature range of 180–300 °C. The hydrochars produced during HTC are spherical and their surface area varies from 1.0–3.5 m^2 g^{-1}, which is very low compared to charcoal or pyrolysis biochar. Therefore, physisorption is highly unlikely but the sequestration of nutrients indicates

chemisorption. FTIR and SEM-DEX provide supporting information on chemisorption. However, the optimum sequestration and kinetics of sequestration in terms of specific nutrients needs to be further investigated.

Acknowledgements

This research is supported by funds from the Bioenergy 2021 program delegated from the German Federal Ministry of Research and Education (BMBF) to Project Management Juelich (PtJ). Additionally, the authors acknowledge Western Sun Grant Initiative (grant no. 2010-38502-21839) for the financial support. The authors also acknowledge the analytical support of Zeta Partikel Analytik, Germany, especially Dr. Andreas Hahn for SEM and nitrogen sorption analyses.

Conflict of interest

All authors declare no conflicts of interest in this paper.

References

1. Reza MT, Lynam JG, Vasquez VR, et al. (2012) Pelletization of Biochar from Hydrothermally Carbonized Wood. *Environ Prog Sustain* 31: 225-234.
2. Reza MT, Lynam JG, Uddin MH, et al. (2013) Hydrothermal carbonization: Fate of inorganics. *Biomass Bioenerg* 49: 86-94.
3. Reza MT, Borrego AG, Wirth B (2014) Optical texture of hydrochar from maize silage and maize silage digestate. *Int J of Coal Geology* 134–135: 74-79.
4. Reza MT, Becker W, Sachsenheimer K, et al. (2014) Hydrothermal carbonization (HTC): Near infrared spectroscopy and partial least-squares regression for determination of selective components in HTC solid and liquid products derived from maize silage. *Bioresource Technol* 161: 91-101.
5. Lynam J, Reza MT, Yan W, et al. (2014) Hydrothermal carbonization of various lignocellulosic biomass. *Biomass Conv Biore*f : 1-9.
6. Coronella C, Lynam J, Reza MT, et al. (2014) Hydrothermal Carbonization of Lignocellulosic Biomass. In: Jin F, editor. *Application of Hydrothermal Reactions to Biomass Conversion: Springer Berlin Heidelberg*: 275-311.
7. Liu ZG, Quek A, Parshetti G, et al. (2013) A study of nitrogen conversion and polycyclic aromatic hydrocarbon (PAH) emissions during hydrochar-lignite co-pyrolysis. *Appl Energ* 108: 74-81.
8. Reza MT, Andert J, Wirth B, et al. (2014) Hydrothermal Carbonization of Biomass for Energy and Crop Production. *Applied Bioenergy* 1: 11-29.
9. Demir-Cakan R, Makowski P, Antonietti M, et al. (2010) Hydrothermal synthesis of imidazole functionalized carbon spheres and their application in catalysis. *Catal Today* 150: 115-118.
10. Bandura AV, Lvov SN (2006) The ionization constant of water over wide ranges of temperature and density. *J Phys Chem Ref Data* 35: 15-30.
11. Reza MT, Yan W, Uddin MH, et al. (2013) Reaction kinetics of hydrothermal carbonization of loblolly pine. *Bioresource Technol* 139: 161-169.

12. Reza MT, Uddin MH, Lynam J, et al. (2014) Hydrothermal carbonization of loblolly pine: reaction chemistry and water balance. *Biomass Conv Bioref* 4: 311-321.
13. Wiedner K, Naisse C, Rumpel C, et al. (2013) Chemical modification of biomass residues during hydrothermal carbonization - What makes the difference, temperature or feedstock? *Org Geochem* 54: 91-100.
14. Funke A (2015) Fate of Plant Available Nutrients during Hydrothermal Carbonization of Digestate. *Chemie Ingenieur Technik* 87: 1713-1719.
15. Heilmann SM, Molde JS, Timler JG, et al. (2014) Phosphorus Reclamation through Hydrothermal Carbonization of Animal Manures. *Environ Sci Technol* 48: 10323-10329.
16. Funke A, Mumme J, Koon M, et al. (2013) Cascaded production of biogas and hydrochar from wheat straw: Energetic potential and recovery of carbon and plant nutrients. *Biomass Bioenerg* 58: 229-237.
17. Heilmann SM, Davis HT, Jader LR, et al. (2010) Hydrothermal carbonization of microalgae. *Biomass Bioenerg* 34: 875-882.
18. Sevilla M, Fuertes AB (2009) The production of carbon materials by hydrothermal carbonization of cellulose. *Carbon* 47: 2281-2289.
19. Funke A, Ziegler F (2010) Hydrothermal carbonization of biomass: A summary and discussion of chemical mechanisms for process engineering. *Biofuel Bioprod Bior* 4: 160-1677.
20. Kruse A, Funke A, Titirici MM (2013) Hydrothermal conversion of biomass to fuels and energetic materials. *Curr Opin Chem Biol* 17: 515-521.
21. Zhu XD, Liu YC, Luo G, et al. (2014) Facile Fabrication of Magnetic Carbon Composites from Hydrochar via Simultaneous Activation and Magnetization for Triclosan Adsorption. *Environ Sci Technol* 48: 5840-5848.
22. Kumar S, Loganathan VA, Gupta RB, et al. (2011) An Assessment of U(VI) removal from groundwater using biochar produced from hydrothermal carbonization. *J Environ Manage* 92: 2504-2512.
23. Regmi P, Moscoso JLG, Kumar S, et al. (2012) Removal of copper and cadmium from aqueous solution using switchgrass biochar produced via hydrothermal carbonization process. *J Environ Manage* 109: 61-69.
24. Hu B, Wang K, Wu LH, et al. (2010) Engineering Carbon Materials from the Hydrothermal Carbonization Process of Biomass. *Adv Mater* 22: 813-828.
25. Demir-Cakan R, Baccile N, Antonietti M, et al. (2009) Carboxylate-Rich Carbonaceous Materials via One-Step Hydrothermal Carbonization of Glucose in the Presence of Acrylic Acid. *Chem Mater* 21: 484-490.
26. Baccile N, Laurent G, Babonneau F, et al. (2009) Structural Characterization of Hydrothermal Carbon Spheres by Advanced Solid-State MAS C-13 NMR Investigations. *J Phys Chem C* 113: 9644-9654.
27. Baccile N, Antonietti M, Titirici MM (2010) One-Step Hydrothermal Synthesis of Nitrogen-Doped Nanocarbons: Albumine Directing the Carbonization of Glucose. *Chemsuschem* 3: 246-253.
28. Zhao L, Bacsik Z, Hedin N, et al. (2010) Carbon Dioxide Capture on Amine-Rich Carbonaceous Materials Derived from Glucose. *Chemsuschem* 3: 840-845.

29. Fechler N, Wohlgemuth SA, Jaker P, et al. (2013) Salt and sugar: direct synthesis of high surface area carbon materials at low temperatures via hydrothermal carbonization of glucose under hypersaline conditions. *J Mater Chem A* 1: 9418-9421.
30. Reza MT, Rottler E, Tolle R, et al. (2015) Production, characterization, and biogas application of magnetic hydrochar from cellulose. *Bioresource Technol* 186: 34-43.
31. Sevilla M, Fuertes AB (2009) Chemical and Structural Properties of Carbonaceous Products Obtained by Hydrothermal Carbonization of Saccharides. *Chem-Eur J* 15: 4195-4203.
32. Titirici MM, Antonietti M (2010) Chemistry and materials options of sustainable carbon materials made by hydrothermal carbonization. *Chem Soc Rev* 39: 103-116.
33. Sevilla M, Fuertes AB (2009) Chemical and structural properties of carbonaceous products obtained by hydrothermal carbonization of saccharides. *Chemistry* 15: 4195-4203.
34. Cao XD, Ma LN, Gao B, et al. (2009) Dairy-Manure Derived Biochar Effectively Sorbs Lead and Atrazine. *Environ Sci Technol* 43: 3285-3291.
35. Diakite M, Paul A, Jager C, et al. (2013) Chemical and morphological changes in hydrochars derived from microcrystalline cellulose and investigated by chromatographic, spectroscopic and adsorption techniques. *Bioresource Technol* 150: 98-105.
36. Si Y, Ren T, Li Y, et al. (2012) Fabrication of magnetic polybenzoxazine-based carbon nanofibers with Fe3O4 inclusions with a hierarchical porous structure for water treatment. *Carbon* 50: 5176-5185.
37. Lynam JG, Reza MT, Vasquez VR, et al. (2012) Effect of salt addition on hydrothermal carbonization of lignocellulosic biomass. *Fuel* 99: 271-273.
38. Ryu J, Suh YW, Suh DJ, et al. (2010) Hydrothermal preparation of carbon microspheres from mono-saccharides and phenolic compounds. *Carbon* 48: 1990-1998.
39. Peterson AA, Vogel F, Lachance RP, et al. (2008) Thermochemical biofuel production in hydrothermal media: A review of sub- and supercritical water technologies. *Energy Env Sci* 1: 32-65.
40. Danso-Boateng E, Shama G, Wheatley AD, et al. (2008) Hydrothermal carbonisation of sewage sludge: Effect of process conditions on product characteristics and methane production. *Bioresource technology* 177: 318-327.

AIMS Press